The Solution Structure of the Hairpin Formed by d(TCTCTC-TTT-GAGAGA)†

Margret M. W. Mooren,‡,§ David E. Pulleyblank,‖ Sybren S. Wijmenga,‡ Frank J. M. van de Ven,‡ and Cornelis W. Hilbers*,‡

NSR Centre for Molecular Structure, Design, and Synthesis, Laboratory of Biophysical Chemistry, University of Nijmegen, Toernooiveld 1, 6525 ED Nijmegen, The Netherlands, and Department of Biochemistry, University of Toronto, Toronto, Ontario, Canada, M5S 1A8

Received January 3, 1994; Revised Manuscript Received April 15, 1994®

ABSTRACT: The 15-residue oligonucleotide d(TCTCTC-TTT-GAGAGA) forms a hairpin structure with a loop of three thymidine residues at neutral pH or above. The three-dimensional solution structure of this oligonucleotide has been determined by means of two-dimensional nuclear magnetic resonance methods. Interproton distance constraints derived from NOEs, in combination with torsion angle constraints obtained from *J*-coupling constants were used in the variable target function program DIANA to derive the hairpin structure. It was found that hairpins with two different loop conformations fit the NMR data, i.e. an equilibrium between these two conformational states can only fully explain the NOE data available. In one state, loop residue T7 is turned into the minor groove, while in the second state residue T8 is in the minor groove. In both conformations the phosphate backbone changes its direction by 180° between residues T9 and G10. Concomitantly, torsion angles ζ of T9 and α of G10 both adopt a gauche(+) conformation and γ of residue G10 adopts a trans conformation to induce this complete change in the direction of the backbone.

The fundamental structural unit in higher order, three-dimensional nucleic acid structures is formed by hairpins consisting of a stem-loop region. For a number of years these units have been the subject of physicochemical studies and by now it is well-established that their stability depends on the length as well as the nucleotide sequence of the loop region. Several attempts have been made to explain this variation in stability in terms of the conformation of the loop region, given of course identical stems. So far, most structural studies were performed on hairpins with an even number of nucleotides in the loop region, among which studies on four-membered loops predominated. In our laboratory elaborate studies were performed on DNA hairpins with four-membered loops. These investigations demonstrated that for certain loop sequences base pairs can be formed between the first and the last base of the loop region. An example is provided by the hairpin formed by d(ATCCTA-TTTA-TAGGAT) in which a T-A Hoogsteen base pair is formed between the first and last base of the loop (Blommers et al., 1991).

In this paper our studies are extended to a hairpin with an odd-membered loop formed by the sequence d(TCTCT-TTT-GAGAGA). The stem of this hairpin consists of complementary homopurine and homopyrimidine strands. Such strands are widely dispersed components of most eukaryotic genomes (Wells et al., 1988). In some cases they may have regulatory functions (Larsen & Weintraub, 1982), by, for example, playing a role in chromosome folding (Johnson & Morgan, 1978) and recombination (Wohlrab et al., 1987). These tracts show an unusual sensitivity to S1 and related single strand specific nucleases at the low pH conditions where these enzymes are active (Lyamichev et al., 1985; Pulleyblank et al., 1985) as well as to superhelical stress. The hairpin studied here may serve as a model of the conformational behavior of such homopurine–homopyrimidine tracts. It was shown earlier by means of one- and two-dimensional ^{1}H-NMR[1] that under neutral or slightly alkaline pH conditions the hairpin form of the molecule d(TCTCTC-TTT-GAGAGA) predominates, while at low pH two hairpin molecules interact so as to form a partially triple helical and partially single-stranded structure (Mooren et al., 1990). Thus, it is interesting to derive more detailed and quantitative structural information for the loop region of d(TCTCTC-TTT-GAGAGA), at these different pH conditions. Here we consider the hairpin formed at pH = 8. The availability of a detailed solution structure of d(TCTCTC-TTT-GAGAGA) also allows for a comparison with results obtained for the hairpins with even-numbered loops studied so far (Blommers et al., 1987, 1989, 1991; Haasnoot et al., 1983a, 1986).

MATERIALS AND METHODS

Experimental. The oligonucleotide d(TCTCTC-TTT-GAGAGA) was purchased in deblocked form from Synthetic Genetics, La Jolla, CA. Purity was checked by electrophoresis on 20% polyacrylamide gels.

NMR samples were prepared by dissolving the 3-fold lyophilized oligonucleotide to a concentration of 2 mM in a solution containing 0.1 M sodium deuterioacetate in water or deuterium oxide. The pH/pD was adjusted to pH/pD = 8.0 (meter reading) by addition of deuterioacetic acid. ^{1}H-NMR spectra of the sample dissolved in D_2O were recorded at a temperature of 298 K, at 400 MHz on a Bruker AM-400

† This work was supported by the Dutch Foundation for Chemical Research (SON) with financial aid from the Netherlands Organization for the Advancement of Research (NWO) and by an operating grant from the Medical Research Council of Canada.

* Author to whom correspondence should be addressed.

‡ University of Nijmegen.

§ Present address: Unilever Research Laboratorium, Olivier van Noortlaan 120, 3133 AT Vlaardingen, The Netherlands.

‖ University of Toronto.

® Abstract published in *Advance ACS Abstracts,* May 15, 1994.

[1] Abbreviations: NMR, nuclear magnetic resonance; NOE, nuclear Overhauser enhancement; NOESY, NOE spectroscopy; 1D, one-dimensional; 2D, two-dimensional; FID, free induction decay; DQF-COSY, double quantum-filtered correlated spectroscopy.

0006-2960/94/0433-7315$04.50/0

spectrometer, interfaced to an ASPECT 3000 computer. Phase-sensitive two-dimensional spectra were obtained using time-proportional phase incrementation (Marion & Wütrich, 1983). NOESY spectra (Jeener et al., 1979) were measured with a spectral width of 4000 Hz, using mixing times of 80, 150, 300, and 700 ms. The spectra were acquired with 2K points in the t_2-direction and 512 points in the t_1-direction. The time domain data in the t_1-direction were zero-filled to 1K points. Prior to Fourier transformation, the spectra were apodized with a Lorentz–Gauss window function in the t_2-direction and with a shifted squared sine bell window function in the t_1-direction. A 600-MHz NOESY spectrum of the sample, dissolved in water, was recorded at 283 K, using a time-shared long pulse as observation pulse (Haasnoot & Hilbers, 1983). The spectral width was 31250 Hz; the carrier was placed at the low-field end of the spectrum. The spectrum was acquired with 4K points in the t_2-direction and 512 points, zero-filled to 1K points, in the t_1-direction; the mixing time was 400 ms. Before Fourier transformation, each free induction decay was subjected to data shift accumulation. Furthermore, a 400-MHz, double quantum-filtered correlation spectrum (DQF-COSY) (Chazin et al., 1986) was recorded with a spectral width of 4000 Hz, and was acquired with 512 points in the t_1-direction and 2K points in the t_2-direction. The time domain data were zero-filled in both directions to 1K and 4K, respectively, and were multiplied with shifted sine bell functions before Fourier transformation.

Conformational Analysis. The conformational analysis of the hairpin was performed according to the following procedure. The conformation of each sugar residue was determined using the experimentally derived J-couplings, $J(1'2')$ and $J(1'2'')$, and the sums of J-couplings:

$$\sum 1' = J(1'2') + J(1'2'')$$

$$\sum 2' = J(1'2') + J(2'2'') + J(2'3')$$

$$\sum 2'' = J(1'2'') + J(2'2'') + J(2''3')$$

which served as the input for the computer program MARC (Blommers et al., 1991), developed to perform a conformational analysis of the deoxyribose conformation. Where possible, the J-couplings $J(1'2')$ and $J(1'2'')$ were derived through the simulation of the 1D spectrum, using the Bruker program PANIC. For the remaining residues, sums of J-couplings were estimated from the multiplet patterns in the recorded DQF-COSY spectrum. The precision of the latter data was low, because of the limited digital resolution.

Interproton distances were calculated with the computer program NO2DI (van de Ven et al., 1991); in a new version of the program, NOEs to rotating methyl groups are accounted for. The program can be obtained from Dr. F. J. M. van de Ven. NO2DI needs the intensities of the NOESY cross peaks as input. These were determined by means of the integration routine running on a Bruker X32 computer. Integration was performed for the NOESY spectra recorded with mixing times of 75, 150, and 300 ms. The NO2DI algorithm first generates so-called "zeroth order" estimates for the distances, which are obtained from the NOEs by using the expression $n_{ab} = C/r_{ab}^6$, in which n_{ab} denotes the intensity of the NOE cross peak between the resonances of protons a and b, C is a scaling factor, and r_{ab} is the distance between protons a and b. From these data a relaxation matrix is constructed to simulate an NOE spectrum. Subsequently, a better estimate for the distance r_{ab} is obtained, via an iterative procedure, by comparing the measured with the calculated NOEs. In this procedure, distances belonging to the most intense NOEs are optimized first, because for these distances spin diffusion is relatively unimportant. The NO2DI calculations were performed for a resonance frequency of 400 MHz and using a rotation correlation time τ_c = 1.8 ns, which was estimated with the aid of the Stokes–Einstein equation (Cantor & Schimmel, 1980). The NOE intensities belonging to the H5–H6 proton pair of the cytosines were used to determine the scaling factor C.

From the intraresidue cross peak intensities and the distances calculated with NO2DI for the proton pairs H6/H8–H1′/H2′/H2″, the glycosidic torsion angle, χ, could be derived. Information about the backbone torsion angle γ was obtained from combined NOE and J-coupling data, i.e. the dependence of the ^{1}H–^{1}H coupling constants $J(4'5')$ and $J(4'5'')$ and the ^{1}H–^{1}H distances of the pairs H3′–H5′, H3′–H5″, H4′–H5′, and H4′–H5″ on torsion angle γ served to estimate the value of γ (Blommers et al., 1991). The torsion angles β and ϵ were determined from heteronuclear J-coupling constants (vide infra).

On the basis of the available NMR constraints, the hairpin structure was derived by means of the variable target function distance geometry algorithm DIANA (Güntert et al., 1991). It proved necessary to change too large bond angles in the program library; e.g. the angle C4′–C3′–O3′, which was 116.5° in the original DIANA dataset, was changed to 109.3° in the new library. Furthermore, the original DIANA algorithm was adapted in our laboratory to incorporate variable sugar puckers; in the original DIANA program the sugar puckers are kept fixed during the calculations. (The program can be obtained from Prof. K. Wüthrich.) The calculations were performed on a CONVEX-C120 computer. Upper and lower distance bounds, as derived from the interproton distances calculated with NO2DI, and the domains estimated for the torsion angles were taken as input for DIANA. Lower bounds were taken equal to the distances derived from NO2DI diminished by 10%; to calculate upper bounds, 20% was added to the NO2DI distances. In the first step, 100 structures were calculated. The input included 24 lower and upper distance constraints for the loop and 120 lower and upper distance constraints for the stem. It is noted in passing that in order to obtain a regular helix for the stem, in addition to the experimental constraints, standard B-type distance constraints (Wüthrich, 1986) and torsion angle domains (Saenger, 1984) were added. These included 30 hydrogen-bond constraints for the six base pairs in the stem; in addition, for each base pair the C1′–C1′ and the N1–N9 distances were constrained (Saenger, 1984) to ensure planarity of the base pairs. Furthermore, for the total molecule, 93 dihedral angle constraints and stereospecific assignments for 20 out of a total of 30 CH_2 groups (H2′/H2″ and H5′/H5″) were added. For each conformation the target function was minimized at levels 0–14, whereby minimization at level 14 was done three times. (The "minimization level" is 0 if exclusively intraresidue distance constraints are considered, 1 if in addition nearest neighbor sequential distance constraints are included, 2 if next nearest neighbors are included, etc.) The weighting factors for the upper and lower distance limits were set to 1.0 and the weighting factor for dihedral angle constraints was set to 5.0. For levels 0–13 and for the first minimization step at level 14, the weighting factor for the van der Waals constraints was 0.5; for the second minimization step at level

14, it was increased to 1.0, and for the final minimization step at level 14, it was increased to 2.0. For the minimization levels 1–13 and for the first step at level 14, the maximal number of target function calculations was set to 100, and for the last two teps at level 14, it was set to 200. The coordinates of the five DIANA structures with the lowest target functions were taken as input for the program CORMA (Keepers & James, 1984), which calculates the dipole–dipole relaxation matrix for a system of protons and converts that into a NOESY spectrum. These calculations showed that for the calculated DIANA structures short interproton distances are generated for proton pairs for which no experimental NOE cross peak was observed, even in NOESY spectra with long mixing times. The absence of an NOE cross peak could either mean that the distance between the protons of the pair is >4 Å or that local motion quenches the NOE intensities. If a number of other intra- or interresidue NOEs involving the mentioned protons contradict local motion, it was assumed that the absence of the aforementioned NOE cross peak was due to a long internuclear distance. Then, for these atom pairs, the lower distance constraint was set to 4 Å and DIANA was run again. Subsequent cycles of DIANA and CORMA were carried out until agreement between the simulated and experimental NOE spectrum was achieved. In the last DIANA run, 400 structures were calculated.

Restrained energy minimizations were carried out on a Silicon Graphics Iris 4D-25G work station, using version 3.2.1 of the program Quanta (Polygen), which uses the CHARMm force field. A distance-dependent dielectric constant was used. 1000 steps of energy minimization were performed with the Adopted Basis Newton Raphson minimization method. Dihedral and distance constraints had the form of a pseudo-square-well potential.

RESULTS

Spectrum Interpretation

Exchangeable Protons. The oligonucleotide studied in this paper forms a hairpin with an odd-numbered loop. To investigate whether it is a three- or a five-membered loop, imino proton spectra were measured at different temperatures, which are shown in Figure 1. Assignment of the resonances was based on a two-dimensional NOE spectrum of a sample, dissolved in H_2O (data not shown). The peak belonging to the terminal base pair is missing, most likely because of fraying effects. One very broad peak of low intensity is seen around 10.5 ppm at 287 K, which belongs to the imino protons of the unpaired residues in the loop region. At higher temperature, this peak broadens beyond detection. From these spectra, it could be concluded that the loop consists of three thymidine residues.

UV melting experiments performed at different concentrations, up to NMR conditions, resulted in a concentration-independent melting temperature of 63 °C, demonstrating that the NMR experiments are carried out on a hairpin molecule. Furthermore, the UV experiments yielded ΔH-values for the hairpin-to-coil transition which are in good agreement with the values expected for a hairpin loop consisting of three residues.

Nonexchangeable Protons. The nonexchangeable base and sugar ring protons of the hairpin were assigned by analysis of the NOESY spectra, recorded in D_2O. Standard sequential assignment procedures are available, relying on networks of short proton–proton distances (Haasnoot et al., 1983; Scheek et al., 1983; Hare et al., 1983).

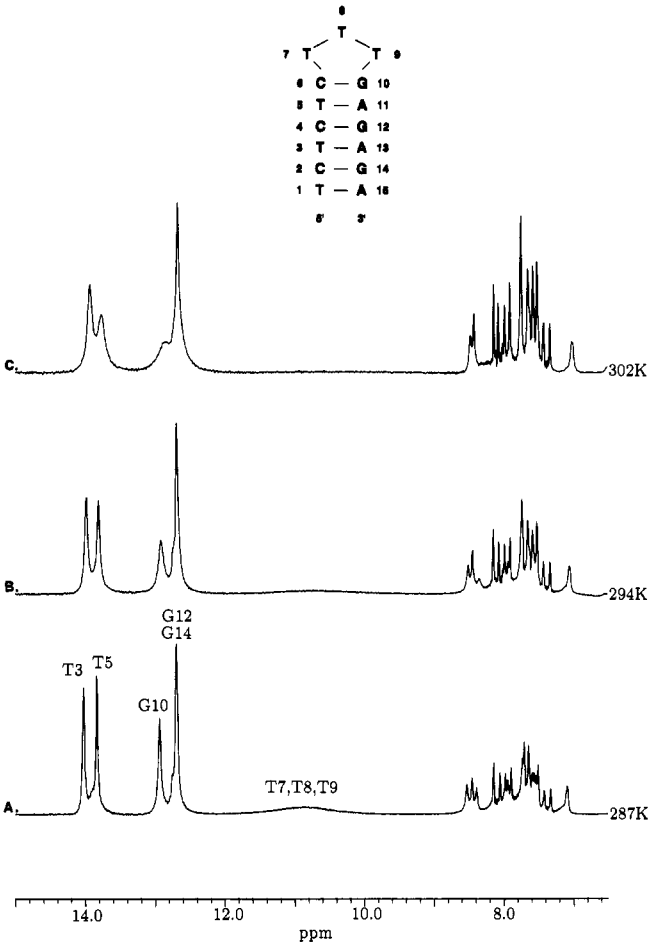

FIGURE 1: 600-MHz imino proton spectrum of the hairpin formed by d(TCTCTC-TTT-GAGAGA) at pH = 8, recorded at 287 K (A), 294 K (B), and 302 K (C).

An expanded contour plot of part of the 300-ms NOESY spectrum of d(TCTCTC-TTT-GAGAGA) is plotted in Figure 2. In this plot connectivities are established between the base protons on one hand and the sugar H1′ and cytidine H5 protons on the other hand. Starting with the H6–H1′ cross peak for residue T1, the ring H6 and sugar H1′ proton resonances can be assigned, until the H1′-resonance of residue T9 in the loop is reached. Subsequently, starting at the 3′-end with the H8–H1′ cross peak of residue A15, a sequential connectivity walk can be made until the H8–H1′ cross peak of G10 is reached. It is not possiible to go one step further, except for longer mixing times, when a very weak peak is observed between G10H8 and T9H1′ (Figure 2). The strongest cross peak intensities correspond to the NOEs between the H6 and H5 protons of the cytidines, with their short, fixed interproton distance of 2.45 Å. The H5–H6 cross peak assignments were confirmed by the appearance of the corresponding J-connectivities in a DQF-COSY spectrum (data not shown). A similar sequential assignment can be obtained for the connectivities between the H6/H8 base- and H2′/H2″ sugar proton resonances, and at the longer mixing times, it is even possible to make a sequential walk based on H6/H8 and H3′ connectivities. The sequential analysis for the H6/H8 and H2′/H2″ resonances cannot, however, be extended into the loop region as far as that for the H1′ resonances.

By combining the H1′–H2′/H2″ NOE cross peaks and the corresponding cross peaks in the DQF-COSY spectrum, it is nevertheless possible to assign all H2′ and H2″ resonances. A stereospecific assignment of the H2′ and H2″ resonances could be achieved for all residues after analysis of the

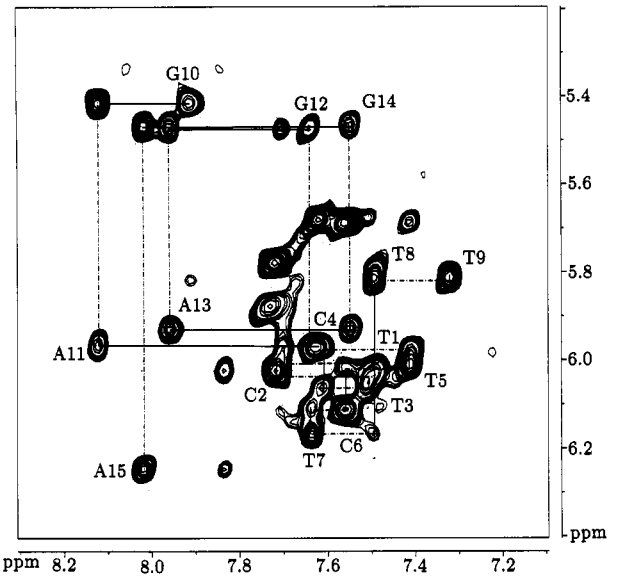

FIGURE 2: Part of the 400-MHz, phase-sensitive, NOESY spectrum of d(TCTCTC-TTT-GAGAGA), dissolved in D_2O, exhibiting cross peaks between aromatic H6/H8 protons and sugar H1′ protons. The spectrum was recorded at a temperature of 298 K for a 2 mM sample at pH = 8 with a mixing time of 0.3 s. The sequential analysis of the spectrum is indicated. The numbering of the resonances corresponds with that in the hairpin in Figure 1. Only the assignments of the intraresidue cross peaks, H6/H8$_i$–H1′$_i$, are given. A small number of nonsequential cross peaks is present in this part of the spectrum; these cross peaks belong to cytosine H5–H6 and to adenine H2–H1′ proton pairs.

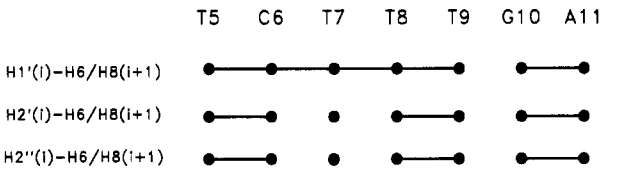

FIGURE 3: Connectivity diagram composed of the sequential NOE cross peaks between H1′$_i$–H6/H8$_{i+1}$, etc., of the residues T5 through G10 (see hairpin structure in Figure 1). A drawn line corresponds with the presence of an unambiguous cross peak. The absence of cross peaks between residues T9 and G10 for all connectivity pathways is noteworthy; the connectivities between C6 and T7 and between T7 and T8 suggest deviations from a B-type conformation.

J-coupling patterns of the cross peaks in the DQF-COSY spectrum and the intensities of the cross peaks in the NOESY spectra obtained at the shorter mixing times. The sequential interresidue connectivities, obtained for the loop residues of the hairpin and the residues which close the loop, are schematized in Figure 3.

At this point, at attempt can be made to assign the remaining resonances to the individual sugars. The final results are given in Table 1. If possible, the assignments were confirmed by means of a TOCSY and a DQF-COSY experiment (data not shown). Because of overlap, a complete identification of the sugar proton resonances could not be achieved for all residues.

A stereospecific assignment of the H5′ and H5″ resonance is necessary to be able to determine the value of torsion angle γ (Wijmenga et al., 1993), but is not possible for all residues. The H5′ as well as the H5″ resonances of residues T9 and G10 could be assigned stereospecifically, but for example, for residues T7 and T8, only one of the resonances, i.e. the H5″ resonance on basis of NOE intensities and *J*-coupling constants, could be assigned, while the position of their corresponding H5′ resonances could not be established.

Table 1: Chemical Shifts of the Nonexchangeable Proton Resonances of d(TCTCTC-TTT-GAGAGA) at 298 K[a]

residue	H6 H8	H1′	H2′	H2″	H3′	H4′	H5′	H5″	H5 CH_3 H2
T1	7.48	6.01	2.22	2.53	4.69	4.11		(3.71)	1.66
C2	7.71	6.03	2.21	2.50	4.79	(4.22)		(4.10)	5.78
T3	7.51	6.07	2.30	2.54	4.88				1.67
C4	7.62	5.98	2.15	2.49					5.68
T5	7.42	6.02	2.05	2.47	4.82	(4.11)	(4.17)	(4.07)	1.68
C6	7.57	6.12	2.21	2.29	4.84	4.20		4.02	5.69
T7	7.64	6.18	2.10	2.32	4.88	4.27		4.00	1.85
T8	7.49	5.82	1.94	2.19	4.60	3.83		3.89	1.72
T9	7.32	5.82	1.92	2.11	4.57	3.64	3.60	3.41	1.61
G10	7.92	5.42	2.66	2.80	4.82	4.26	3.98	3.88	–
A11	8.12	5.97	2.65	2.82	5.01	4.39		(4.07)	(7.70)
G12	7.64	5.47	2.48	2.62	4.96	4.28		(4.12)	–
A13	7.96	5.93	2.49	2.72	4.98	4.35	(4.13)		(7.70)
G14	7.55	5.48	2.37	2.51	4.90				–
A15	8.02	6.25	2.51	2.40	4.61	4.20	(4.14)	(4.08)	7.83

[a] The chemical shifts, given in ppm, are relative to DDS. The assignments given between parentheses are preliminary. The empty places refer to nonassignable resonances.

Table 2: *J*-Coupling Constants and Sums of *J*-Coupling Constants Obtained for the Sugar Rings[a]

residue	$J(1'2')$	$J(1'2'')$	$\Sigma 2'$	$\Sigma 2''$	P_S	ϕ_{mS}	x_S
T1							
C2							
T3	10.5*	5.1*	25.9*		162–203	38–42	0.75–1.00
C4	8.1	6.7	28.8*	24.9*	117–162	32–42	0.60–0.70
T5	9.8*	4.9*	29.3*	23.4*	122–176	36–42	0.75–0.85
C6	7.2	7.2	28.8*	21.7*	180–207	32–36	0.85–1.00
T7	7.3	6.7	24.9*	22.0*	198–207	36–42	0.80–0.85
T8	7.3	6.7	24.4*	21.0*	176–207	32–42	0.75–0.90
T9	7.3	6.7	24.4*	22.0*	180–207	36–42	0.70–0.85
G10	9.5	6.5	28.8*		153–185	32–36	0.85–1.00
A11	7.3	6.7			117–207	32–42	0.55–1.00
G12	10.3*	4.9*	25.9*		167–203	40–42	0.80–1.00
A13	8.1	6.9	27.3*	21.6*	203–207	34–38	0.95–1.00
G14	10.7*	3.4*	27.8*	20.5*	149–171	42	0.90–1.00
A15	7.0	6.8	28.3*	22.5*	194–207	32–34	0.85–0.95

[a] The couplings marked with an asterisk have been deduced from cross sections through the multiplets in a DQF-COSY spectrum and the unmarked coupling constants have been derived by simulation of the 1D-proton spectrum (see text). Empty places indicate that the corresponding parameters could not be determined. The pseudorotational parameters, P and ϕ_m, of the sugar were obtained by MARC analysis (Blommers et al., 1991). P_S was sampled between 117° and 211.5° in steps of 4.5°, ϕ_{mS} was sampled between 32° and 42° in steps of 2° and the molar fraction, x_S, was sampled between 0.0 and 1.0 in steps of 0.05.

Torsion Angle and Distance Constraints

The pseudorotation parameters, P_S and ϕ_{mS} and the fraction of the S-type puckered sugar, x_S, derived by means of the conformational analysis program MARC (Blommers et al., 1991) (see Materials and Methods) are listed in Table 2. Because of the limited accuracy of the *J*-coupling data, the resulting domains of the angles of pseudorotation are not very narrow and in some instances neither are those of the fractions x_S. It follows, however, that the S-type pucker is the predominant conformation for all sugars. In this report it is noted that for the loop residues T7, T8, and T9, the fraction of the S-type sugar is high but never reaches a value of 1.0. Furthermore, for the purine strand the S-pucker seems more dominant than for the pyrimidine strand. Because S-type sugars are predominant, the corresponding puckering parameters were used in the structure calculations.

The intraresidue distance between the H6/H8 and H1′ protons depends on χ only. If an equilibrium is present between

N- and S-puckered sugars and if it is assumed that torsion angle χ of the N-type sugars is equal to χ of the S-type sugars, then the H6/H8–H1′ distances, calculated with NO2DI, indicated that χ is in the anti region between 170° and 260° for all residues in the hairpin. If it is assumed that χ in a nucleotide with N-type sugars is about 50° lower than in S-type sugars, i.e. $\chi_N = \chi_S - 50$, then the measured distance d_i(H6/H8;H1′) depends on χ_N/χ_S and through this on the percentage N- or S-type sugars. In this situation, the range available for χ becomes larger, with χ between 120° and 280°.

The determination of the remaining backbone torsion angles involves the combined use of NOE- and J-couplings data. Torsion angle β is monitored by the H5′P and H5″P J-coupling constants. In A- and B-type helical structures β is found in the trans domain. If β is exactly equal to 180°, both J(H5′P) and J(H5″P) are small, i.e. about 2 Hz (Mooren, 1993). If β adopts a value around 210°, as is the case in B-DNA, J(H5″P) will be about 7 Hz and a distinct cross peak should appear in a proton–phosphorus correlation spectrum, while J(H5′P) remains very small and no cross peak can be detected. Because of severe overlap in the ^{1}H–^{31}P heterocorrelated spectrum, no assignments can be made and consequently the values of the J-coupling constants cannot be estimated from this spectrum. In the case where β adopts a gauche(–) or gauche(+) conformation, J(H5′P) or J(H5″P) may increase to about 23 Hz (Mooren, 1993). This should be apparent in a DQF-COSY spectrum as a large passive coupling constant. For the sufficiently well-resolved H5′ and H5″ cross peaks in the stem as well as the loop, such large couplings were not observed, which indicates that β adopts a trans conformation for the corresponding residues.

On the basis of sterical grounds, torsin angle ϵ may only adopt trans or gauche(–) values (unpublished results). If ϵ is in the gauche(–) conformation and the sugar is in a C2′-endo conformation, the four bonds H2′–C2′–C3′–O3′–P lie in the same plane and form a W-shaped conformation (Sarma et al., 1973). One may then expect to observe a long-range coupling, J(H2′P3). In the ^{1}H-^{31}P heterocorrelated spectrum cross peaks between H2 and P3, which are normally smaller than 2.7 Hz (Sarma et al., 1973), are not observed. Therefore it was assumed that all torsion angles ϵ fall in the trans domain.

Torsion angle γ of the loop residues was determined using the assignments of the H5′ and H5″ resonances, in a way already described earlier (Wijmenga et al., 1993). The γ angle of loop residues T7, T8, and T9 resides in the normal gauche(+) range; the J(4′5″) couplings are so small that no cross peaks are observed in the COSY spectrum. On the other hand, the γ angle of residue G10 falls in the trans domain. This follows from the NOESY spectrum (Figure 4A) in which reasonably strong NOEs of comparable intensity are observed between the H3′ and H5′/H5″ proton pairs of G10. Furthermore, in the DQF-COSY spectrum the G10 H4′–H5″ multiplet shows a splitting by a large active coupling of about 9 Hz (Figure 4B). Torsion angles α and ζ cannot be determined from J-coupling constants. Theoretical calculations demonstrate, however, that on the basis of sterical grounds, both torsion angles may not adopt values between –30° and 30° (unpublished results).

The NOE connectivities which form the basis for the structure determination of the loop region are schematized in Figure 5. The experimental cross peak intensities as well as the upper and lower bounds for the distances and torsion angles as used in DIANA are listed in Table 3. The connectivity patterns observed for the dinucleotide steps in the loop indicate that the nucleotide chain strongly deviates from a standard

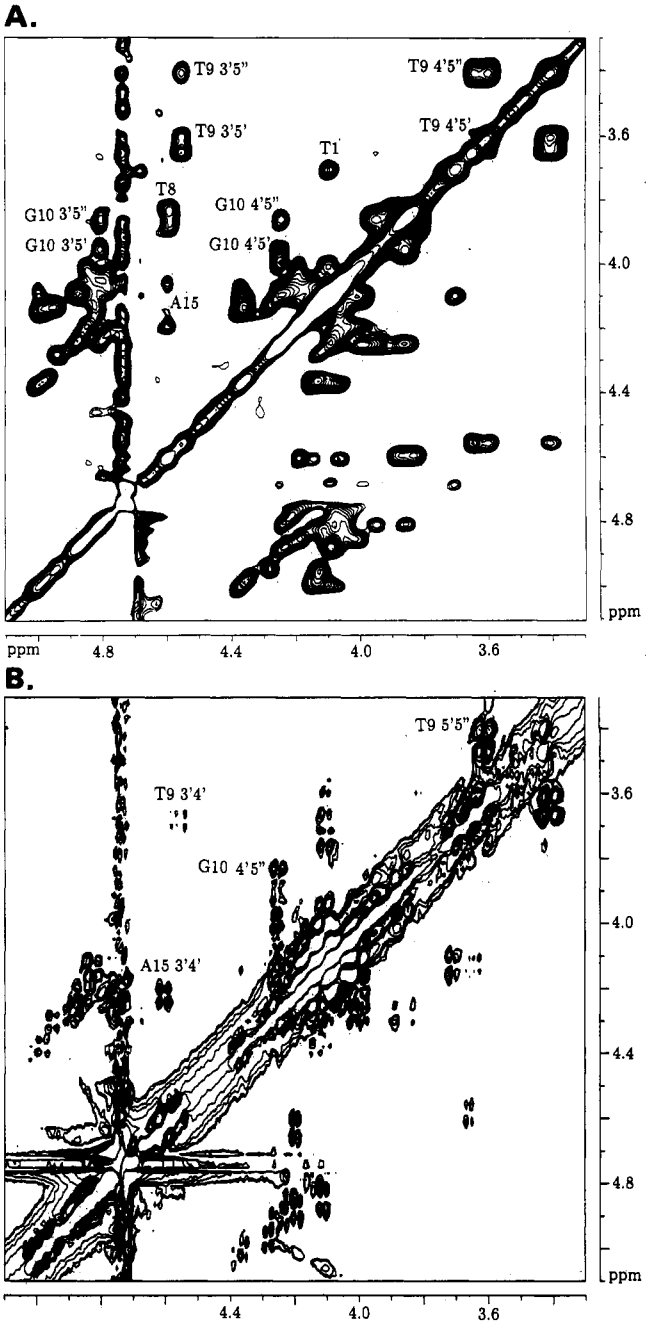

FIGURE 4: (A) Part of the 400-MHz NOESY spectrum of d(TCTCTC-TTT-GAGAGA), recorded with a mixing time of 0.3 s. The region in which the H3′, H4′, and H5′/H5″ resonances are found is shown. The cross peaks corresponding to intranucleotide NOEs of residue G10 are indicated. (B) The corresponding part of the 400-MHz DQF-COSY spectrum. The cross peak patterns of G10 are indicated again. The indicated NOEs and J-coupling patterns are used in the determination of torsion angle γ of G10, as described in the text.

B-DNA type conformation. In the C6–T7 step the cross peak between C6H1′ and T7H6 as well as the cross peaks between C6H2′/H2″/H5 and the methyl group of T7 reflect the normally observed pattern. On the other hand, reasonably intense NOEs normally found in standard B-DNA between CH2′/H2″ and TH6 of residues C6 and T7, respectively, are absent, even at longer mixing times. Additionally, nonstandard cross peaks are observed between C6H1′ and T7H2′ and between C6H4′ and T7CH_3 (CH_3 = methyl group), indicating that the C6–T7 step deviates from that in the normal B-type helix. Although weak, two interesting long-range contacts are observed between C6H1′–T8CH_3 and C6H2″–T8CH_3,

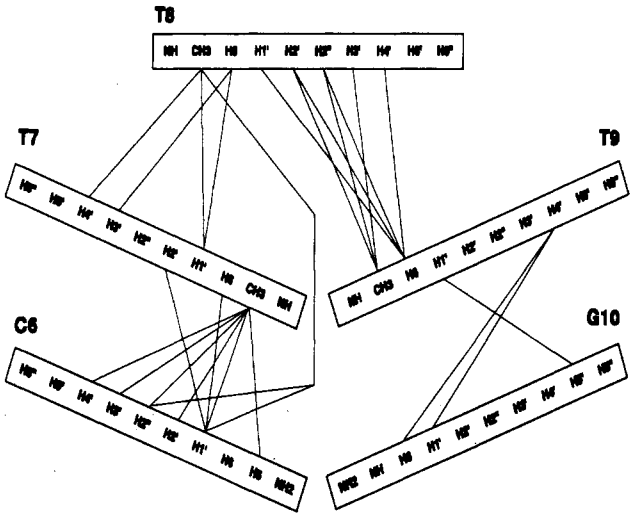

FIGURE 5: Schematic representation of the connectivities observed between the protons in the loop region of the hairpin d(TCTCTC-TTT-GAGAGA). Connectivities are indicated by lines connecting the protons in the different residues.

respectively. The connectivities between the spins of residues T7 and T8 show interesting similarities with those observed between the spins of C6 and T7. Again, an Overhauser effect is observed between the T7H1′ and the T8H6 resonance, but the cross peaks between the T7H2′/H2″ and the T8H6 resonances are absent. Although of smaller intensity than the C6–T7 dinucleotide step, a nuclear Overhauser effect is also observed between T7H4′ and T8CH_3. Apart from this T7H4′–T8CH_3 and an additional T7H1′–T8CH_3 cross peak, no other connectivities between protons of residue T7 and the methyl group of T8 are observed. For the T8–T9 step standard B-type connectivities are found, but between the resonances of residues T9 and G10, no standard sequential cross peaks could be observed at all. The well-defined cross peaks observed in the T9–G10 dinucleotide step are T9H4′–G10H1′ and T9H4′–G10H8, respectively.

Structure Determination

The available NOE cross peak intensities were transferred into interproton distances using the program NO2DI; these served to define the distance constraints (see Table 3).

The distance constraints, together with the determined torsion angle domains and sugar pseudorotation parameters, served as input for the distance geometry calculations with the program DIANA (Güntert et al., 1991). Analysis of the 20 structures with smallest target function values showed that the output consists of two classes of conformations. For each of these calculations, the resulting DIANA structure with lowest target function is shown in Figure 6. The torsion angles derived for the loop residues of these structures are presented in Table 4. In the conformation that occurs most abundantly, residue T8 is folded into the minor groove (Figure 6B). This is accompanied by a change of torsion angle α of T8 from the normal α gauche(−) to the unusual α trans state. A change of α to a trans value shortens the distance between the phoshorus atoms P9 and P10, which is necessary for loop closure. The base of residue T7 is tilted with respect to the B-type stem. The base of residue T9 lies above the base of G10 in a more or less parallel orientation, although the distance between the two base planes is longer than what is normal for two reisudes directly stacking on each other. Between T9 and G10, a 180° change in the propagation direction of the phosphate backbone is observed. This turn involves a ζ gauche(+) and an α gauche(+) torsion angle between T9 and G10. Torsion angle γ of G10 adopts a trans conformation, as was deduced from the NMR data.

Table 3: Distance Constraints for the Loop Residues and Torsion Angle Constraints as Used in the Final DIANA Calculations

A. Distance Constraints[a]

involved	atoms	lower bound, Å	upper bound, Å
C6H1′	T7H6	3.10	4.20
C6H1′	T7CH_3	3.50	5.00
C6H3′	T7CH_3	4.10	6.00
C6H4′	T7CH_3	*	*
C6H5	T7Me	4.50	6.40
C6H1′	T7H2′	*	*
C6H2′	T7CH_3	3.20	5.00
C6H2″	T7CH_3	3.20	5.00
C6H1′	T8CH_3	5.00	6.00
C6H2″	T8CH_3	3.50	6.00
T7H1′	T8H6	3.00	6.00
T7H3′	T8H6	3.00	6.00
T7H1′	T8CH_3	3.50	6.00
T7H4′	T8CH_3	2.80	4.90
T8H1′	T9H6	2.70	3.80
T8H2′	T9H6	2.70	3.80
T8H2″	T9H6	3.50	4.90
T8H4′	T9H6	3.20	6.00
T8H2′	T9CH_3	3.50	4.80
T8H2″	T9CH_3	3.70	4.90
T8H3′	T9CH_3	2.80	4.80
T9H4′	G10H8	3.20	5.40
T9H4′	G10H1′	3.40	6.00
T9H1′	G10H5′	3.20	6.00

B. Torsion Angle Constraints[b]

		C6	T7	T8	T9	G10	stem
α	lb		30	30	30	30	−85
	ub		330	330	330	330	−45
β	lb		160	160	160	160	160
	ub		200	200	200	200	220
γ	lb	30	30	30	30	140	30
	ub	70	90	90	90	220	70
P	lb	140	140	140	140	140	140
	ub	190	190	190	190	190	190
ϵ	lb	180	180	180	180	180	180
	ub	250	250	250	250	250	240
ζ	lb	30	30	30	30	30	−115
	ub	330	330	330	330	330	−75
χ	lb	−160	−180	−180	−180	−160	−160
	ub	−90	−90	−90	−90	−90	−90

[a] The lower bounds, equal to 4 Å (see text), are not incorporated in this table. The C6H2′–T7CH_3, C6H2″–T7CH_3, C6H2″–T8CH_3, and T8H2″–CH_3 cross peaks were clearly present in the spectrum, but could not be integrated due to partial overlap. The distance constraints for these atom pairs were chosen in a wide range. An asterisk (*) means that the distance constraint is omitted from the DIANA input after performance of the first CORMA calculations, because the distance found in one type of hairpin is much larger than expected on the basis of the NOE intensity, while in the other hairpin it is much smaller (see text). [b] lb means lower bound and ub the upper bound.

In the second conformation, residue T7 is folded into the minor groove (Figure 6A). This conformation is observed only five times among the 20 structures with the lowest target function values. The observed domains occupied by the torsion angles in these five structures are broader than those observed for the conformations in which T8 is folded into the minor groove. The torsion angles α of T7 and T8 occur in a very broad trans/gauche(−) domain and the torsion angle ζ of C6 occurs in a broad trans domain. These torsion angle conformations allow the base of residue T7 to swing into the minor groove. The base of residue T8 is then turned into the direction of the major groove without connection with any other residue, because the phosphate backbone has to change direction after this residue. Again, the base of T9 lies above

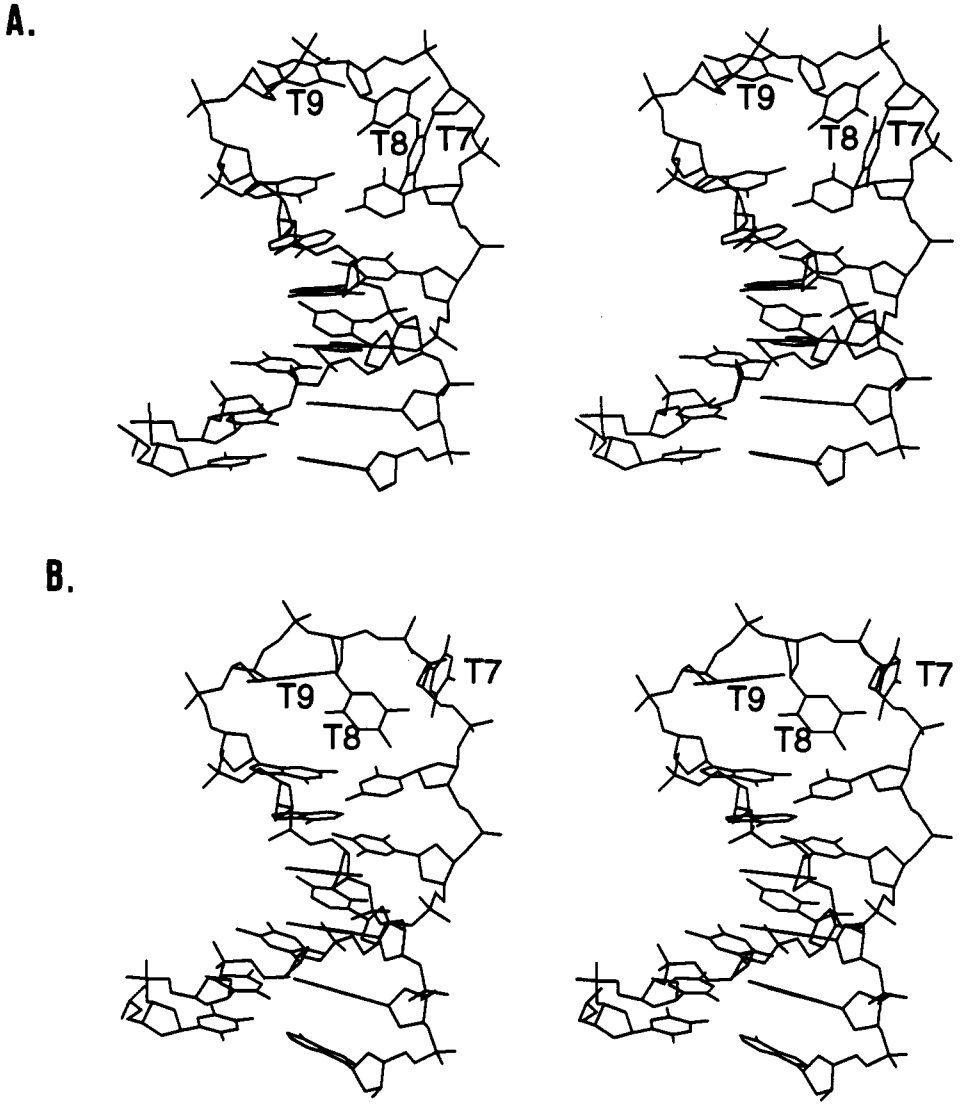

FIGURE 6: Stereoviews of the hairpin models, as obtained via the DIANA calculations. The structures are displayed in the form of stick models. (A) the base of residue T7 is folded into the minor groove; (B) the base of residue T8 is folded into the minor groove.

Table 4: Values of the Torsion Angles of the Loop Structures in the T7- and T8-Hairpin with Lowest Final Target Functions Obtained after DIANA Calculations[a]

residue	α	β	γ	δ	ϵ	ζ	χ	P	ϕ_m
Residue T7 in the Minor Groove									
C6				159	−145	160	−104	191	38
T7	161	−160	74	164	−167	−82	−87	215	38
T8	−106	180	92	132	−172	−105	−127	141	38
T9	−82	−161	90	160	−118	69	177	195	38
G10	85	−158	−140	151			−90	170	39
Residue T8 in the Minor Groove									
C6				137	−174	−131	−91	147	39
T7	−34	172	90	164	−119	147	177	215	39
T8	−176	159	43	147	−160	−112	−154	163	39
T9	−59	169	94	164	−116	91	179	215	39
G10	81	−157	−140	144			−109	158	39

[a] The T7- and T8-hairpins are depicted in Figure 6.

G10 in a more or less parallel orientation at a distance too long for the bases to stack upon each other. The 180° change in the direction of the phosphate backbone is observed between residues T9 and G10 and occurs in the same way as described for the conformation with T8 in the minor groove: ζ as well as α between T9 and G10 adopt a gauche(+) conformation and γ of G10 a trans conformation. All other torsion angles retain their regularly preferred values.

The hairpin in which the base of residue T7 is turned into the minor groove (henceforth referred to as the T7-hairpin) as well as in the hairpin in which the base of T8 is in the minor groove (henceforth referred to as the T8-hairpin) do not (and cannot) at the same time fulfill all of the NMR constraints. Consideration of the data after NOE back-calculation with CORMA indeed showed that the intensity of the NOE connectivity between the resonances of C6H4′ and T7CH_3 as calculated for the T7-hairpin is (much) larger, while for the T8-hairpin it is (much) smaller than experimentally determined. The same holds for the NOEs C6H1′–T7CH_3, T7H2′–T8H6, C6H1′–T7H2′, and T8H4′–T9H6. On the other hand, the intensities calculated for the cross peaks between T7H4′–T8CH_3 and T7H5′/H5″–T8CH_3 in the T8-hairpin are too large, compared with experimental data, and are too small for the T7-hairpin. Since during the sampling procedure we could not find conformations which fulfilled all NMR constraints at the same time, we assumed that these data imply the existence of a fast equilibrium, on the NMR time scale, between the two conformations.

Besides the mentioned violations, which may be explained by the existence of an equilibrium between the T7- and T8-hairpin, both conformations exhibit only one violation larger than 0.2 Å. This concerns the distance between T8H2″ and T9H6 for which the intensity of the connectivity, as calculated

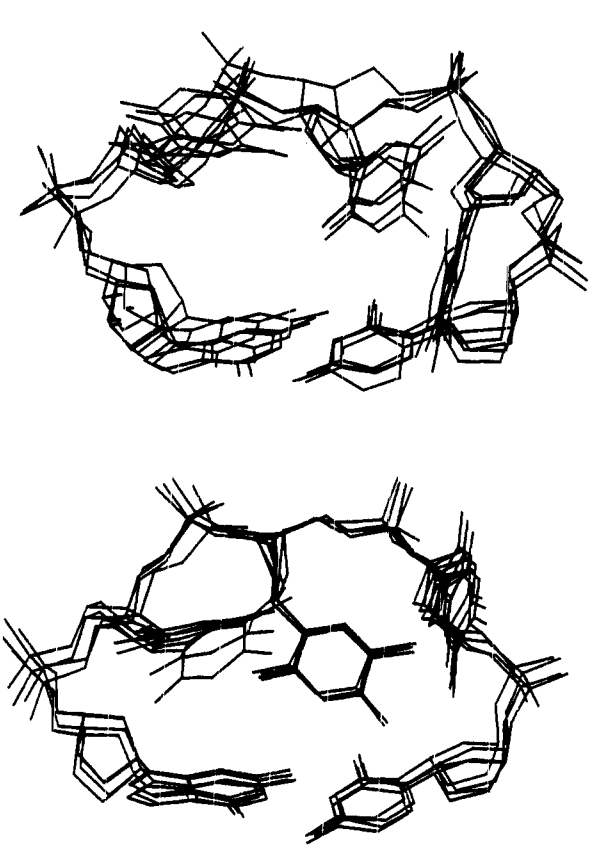

FIGURE 7: (A) Superposition of the loop residues of the four DIANA structures with smallest target function in which residue T7 is folded into the minor groove. The overall root mean square deviation after superposition was 0.9 Å. (B) Superposition of the loop residues of the 10 DIANA structures with smallest target function in which residue T8 is folded into the minor groove. The overall root mean square deviation after superposition was 0.7 Å.

with CORMA for the two models, is 0.04, while that found by integration of the NMR data is only 0.01. At this point we have no explanation for the very low intensity of this connectivity. An impression of the conformational space, occupied by the loop residues of the T7- and T8-hairpin, is presented in Figure 7. The four best T8 hairpin loops (Figure 7B) and the four best T7-hairpin loops (Figure 7A) have been superimposed. The overall root mean square deviation between the conformations in one family is 0.7 and 0.9 Å, respectively. It can be seen that the loop is well-defined, although the T8-hairpin, in which residue T8 is bulged out, is better defined than the T7-hairpin in which residue T7 is bulged out.

DISCUSSION

Conformational Aspects of the Three-Membered Loop. Hairpins, for which so far detailed structural studies have been performed, mainly contained an even number of residues in the loop region. Details of the loop folding depend on, among other things, the base sequence of the loop; e.g. local optimization of the hairpin structure may involve base stacking in the loop or even base pairing of the two terminal nucleotides within a four-membered loop (Blommers et al., 1989, 1991). In this paper, the structure of the pentadecanucleotide d(TCTCTC-TTT-GAGAGA), which forms a hairpin with an odd number of residues in the loop, has been derived. The most surprizing aspect of this study is that a consistent description of the experimental data can only be obtained when two hairpin loop structures are present in solution. The major part of the experimental NOE connectivities shows an excellent fit for both structures, the T7- as well as the T8-hairpin. About seven NOE cross peaks, however, appear in the spectrum, owing to the presence of short interproton distances in only one of the conformers. After the DIANA calculations, restrained energy minimizations were performed. Distance constraints were only used for the NOE connectivities, which were found to belong to a given type of hairpin (i.e. T7- or T8-hairpin) to be energy minimized. After restrained minimization, the energy of the T8-hairpin was 2 kJ/mol lower than that of the T7-hairpin. The torsion angles adopted by both conformations after minimization do not differ by more than 20° from the values obtained after the DIANA calculations; in other words, they remain in the same staggered domains.

Table 5: Torsion Angles, Obtained for Four Oligonucleotide Hairpins at the Position of the 180° Turn in the Direction of the Phosphate Backbone, Compared to the Values Found in Standard B-DNA[a]

oligonucleotide	ϵ	ζ	α	β	γ	ref
d(TCTCTC-TTT-GAGAGA)	t	+	+	t	t	this paper
d(ATCCTA-TTTA-ATCCTA)	–	+	+	t	t	Blommers et al., 1991
cd(ApAp)	t	+	+	t	+	Blommers et al., 1988
d(GGATCG-TTT-CGATCC)	t	+	+	t	t	Boulard et al., 1991
B-DNA	t	–	–	t	+	

[a] These torsion angles are found between the residues depicted in bold. The values of the torsion angles are indicated with the classical rotamers gauche(+), trans, and gauche(–).

When the loop region of the T7- and T8-hairpin is considered and the hairpin is viewed from the top along the helix axis, the course of the sugar phosphate backbone in the 5′-direction is essentially as if it were part of a B-type helix, despite the fact that either T7 or T8 has turned into the minor groove (see Figure 8).

When the T7 base is in the minor groove, the orientation of torsion angle α of T7 has changed from the normal (B-DNA) gauche(–) to the trans (anti) region. The direction of the backbone does not change, however. This is achieved by small compensations of ϵ-C6, ζ-C6, γ-T7, and ϵ-T7. When T8 is found in the minor groove, α-T8 is found in the trans region. Again the direction of the backbone is maintained, now by small adaptations of α-T7, γ-T7, ϵ-T7, and ζ-T7. Between residues T9 and G10, the sugar–phosphate backbone makes a sharp turn in the T7- as well as the T8-hairpin. After this turn, the backbone continues with a standard B-type conformation. Considerations of the backbone torsion angles between residues T9 and G10 shows that they are essentially the same in the T7- and T8-hairpins (see Table 4).

Comparison with Other Hairpins. It has been noted before that a conversion to the ζ gauche(+)/α gauche(+) domain can induce a complete change in the direction of the phosphate backbone (Blommers et al., 1988; Blommers et al., 1991). This is illustrated by the values of the backbone torsion angles obtained for the circular dinucleotide d(ApAp) (see Table 5). The patterns, described above for the torsion angles, involved in the sharp change in the direction of the sugar phosphate backbone have with some variations been observed in a number of other hairpins. The results are summarized in Table 5.

For instance, the $\zeta(+)\alpha(+)\beta(t)\gamma(t)$ combination found for d(TCTCTC-TTT-GAGAGA) has been observed in several other hairpins. Molecular dynamics simulations have shown that combinations like $\zeta(+)\alpha(-)\beta(+)\gamma(t)$, which were obtained by NMR for a small hairpin (Pieters et al., 1989), easily

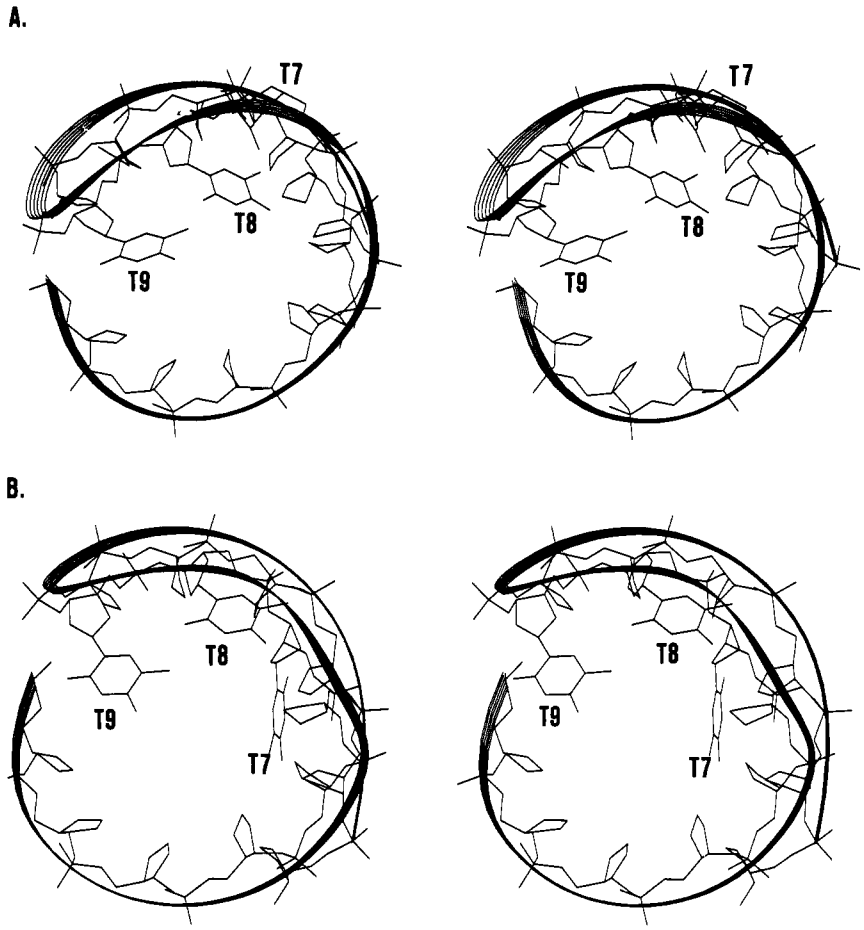

FIGURE 8: Plot of the hairpin structures of the T7-hairpin (A) and T8-hairpin (B) viewed along the helix axis. For clarity, the bases of the stem have been deleted. The direction of the phosphate backbone changes 180° between residues T9 and G10. Note the positions of residues T7 and T8, respectively.

convert to $\zeta(+)\alpha(+)\beta(t)\gamma(t)$, suggesting that the last mentioned combination of torsion angles is energetically very favorable.

In the given examples, torsion angle β is in the trans conformation in all loops. Torsion angle ϵ at the 5′-side of the mentioned torsion angles adopts gauche(−) as well as trans values. In the hairpin d(ATCCTA-TTTA-TAGGAT) (referred to as TTTA-hairpin) (Blommers et al., 1991), ϵ of the third thymidine residue in the loop is in the gauche(−) domain, which allows this residue to stack upon the adenosine in the loop. In the hairpin d(ATCCTA-TTTT-TAGGAT) (referred to as TTTT-hairpin) (Blommers et al., 1987), ϵ of the third loop residue is found in the trans region. This thymidine is partially stacked upon the second loop residue so that the third and fourth bases are kept about 7 Å apart from each other. This situation is comparable with that in d(TCTCTC-TTT-GAGAGA). Torsion angle ϵ of residue T9 adopts a (−)anticlinal conformation preventing T9 from directly stacking upon G10.

In the T8-hairpin the folding of the base of T8 into the minor groove takes place in a way comparable with that observed for the second thymidine in the TTTA-hairpin. In the T7-hairpin, the folding of the base of T7 into the minor groove may be compared with the folding of the second thymidine in the TTTA-hairpin.

Not only are the torsion angle ranges comparable but the observed NOE connectivity patterns are also very similar. The connectivities found in d(TCTCTC-TTT-GAGAGA) between residues C6 and T7 are analogous to those found in the TTTA-hairpin between the first and second thymidine in the loop. In both cases, a nuclear Overhauser effect is observed between the H1′ resonance ($H1'_i$) and the H6 resonance of its 3′-neighbor ($H6_{i+1}$), while the cross peaks between H2′/H2″$_i$ and $H6_{i+1}$ are absent. In both hairpins, a remarkable cross peak is observed between $H1'_i$ and $H2'_{i+1}$, indicating that the nucleotide chains clearly deviate from standard A- or B-type helices. In addition, a cross peak is observed between $H4'_i$ and $CH3_{(i+1)}$. With the exception of the $H1'_i$–$H2'_{i+1}$ NOE, this cross peak pattern repeats itself in the hairpin d(TCTCTC-TTT-GAGAGA) between loop residues T7 and T8. Since in the T7- and T8-hairpin the bases T7 and T8 reside in the minor groove, respectively, this suggests that these observed connectivities between residues i and $i+1$ are typical for a conformation in which residue $i+1$ is folded into the minor groove.

The hairpin d(GGATCG_9-$T_A$$T_B$$T_C$-$C_{13}$GATCC), studied by NMR and molecular mechanics by Fazakerley and coworkers, also contains a loop of three thymidines (Boulard et al., 1991). A comparison of the connectivities observed between the last residue of the stem, G_9, and the first residue in the loop, T_A, shows several similarities with the cross peak patterns mentioned above; i.e. the cross peaks $H1'_i$–$H6_{i+1}$, $H1'_i$–$H2'_{i+1}$, and $H4'_i$–$CH3_{(i+1)}$ are observed between G_9 and T_A as well. In addition, however, the cross peaks $H2'_i$/$H2''_i$–$H6_{i+1}$ are present, which are absent in the d(ATCCTA-$T_7$$T_8$$T_9$$A_{10}$-TAGGAT) and d(TCTCTC-TTT-GAGAGA) spectra. Furthermore, the NOE cross peak $H3'_i$–$CH3_{(i+1)}$ has a larger intensity than the NOE $H4'_i$–$CH3_{(i+1)}$. Despite these differences, it may be expected that the conformation of the dinucleotide step G_9–T_A resembles the C6–T7 and T7–

T8 steps in d(TCTCTC-TTT-GAGAGA) and the T_8–T_9 step in the TTTA-hairpin. Indeed, examination of the family of conformations satisfying the distance constraints for the incorporation of the first T residue on the G–C base pair of the stem of d(GGATCG-TTT-CGATCC) and of the final stereoscopic views confirmed the suggestion that on the basis of this special set of experimental NOEs residue T_A is folded into the minor groove. The 180° change in the direction of the phosphate backbone of this hairpin is also defined by a $\zeta(+)\alpha(+)\beta(t)\gamma(t)$ combination (Table 5). The position of this turn is between residues T_C and C_{13}, which is the same position as found for the presently studied hairpin. A major difference between the two hairpins with three thymidines in the loop concerns the conformation around the torsion angles γ. For d(TCTCTC-TTT-GAGAGA) γ adopts a gauche(+) conformation for all residues except G10. In the model derived for d(GGATCG-$T_AT_BT_C$-CGATCC), γ of each residue T_A, T_B, T_C, and C13 is in the trans domain. Due to spectral crowding, measurement of $J(4'5')$ or $J(4'5'')$ was not possible for the latter molecule; the γ values deduced for T_A and T_B were indicated by the observed NOEs, and those for T_C and C13 were imposed by the loop closure during model building.

Another DNA hairpin with three thymidines in the loop region, d(CGATCG-$T_AT_BT_C$-CGATCG), was studied very recently (Baxter et al., 1993). The reported structure is quite different from the one reported in this and Boulard's paper (Boulard et al., 1991).

Loop Folding. If we compare the various DNA hairpins studied so far in sufficient detail, it stands out that the sharp turn in the sugar phosphate backbone in the loop occurs at the same position for all of these molecules. The turn is found between the last 3′-residue of the loop and the 3′-residue of the base pair closing the loop. It will be interesting to see whether in future studies of other hairpins this will be a common feature of loop folding.

With the present experiments, the list of DNA hairpins in which one of the thymidines in the loop is turned into the minor groove has been extended by another example. As has been mentioned, the surprising result of this study is that either T7 or T8 may exhibit this behavior. General conclusions as to the reason why loop thymidines fold into the minor groove cannot be made at this point. It is interesting though that in hairpins where this effect is observed it is the first thymidine following the 5′-nucleotide of the base pair closing the loop. The hairpin studied in this chapter forms an exception in that not only the first but also the second thymidine after the 5′-nucleotide of the base pair closing the loop may turn into the minor groove. It is noted in passing that examples of hairpin structures are known where these central thymidines do not turn into the minor groove (Blommers et al., 1987; Orbons et al., 1986, 1987). At this moment, it is not at all clear why this happens in one hairpin and not in the other. There are some indications that the thymidine in the minor groove may be stabilized by hydrogen bonds.

In this respect it is interesting to recall the loop-folding principle, introduced earlier (Haasnoot et al., 1986), which was based on the assumption that the stacking of the bases in the stem is continued in the loop region. The preceding discussion demonstrates that this does not hold up with respect to the stacking of the bases but it does for the course of the backbone including the position of the sharp turn changing its direction. Further investigations are called for to be able to relate these observations. Several hairpins with a loop of four residues have been studied. The results have shown that under specific conditions the terminal bases of the intervening loop sequence are involved in some kind of base pairing (Blommers et al., 1987, 1991; Pieters et al., 1989). The data presented in this paper deal with a hairpin loop that consists of three thymidines. The loop is closed by a C-G base pair. In this three-membered loop, the phosphate backbone propagates in a normal way on top of the 3′-end of the B-type double helical stem, while after the third residue the backbone changes its direction, as expected on basis of the original folding principle. The data presented for a different three-membered hairpin loop, which is closed by a G-C base pair (Boulard et al., 1991), also suggest that the rather simple model of folding is followed.

CONCLUSION

The stable hairpin with three membered loop, d(TCTCTC-TTT-GAGAGA), is flexible under the used experimental conditions. On the NMR time scale, a fast equilibrium exists between a conformational state in which residue T7 is in the minor groove and a conformational state in which residue T8 is in the minor groove. The NOE data have been described and explained in a qualitative way. The hairpin has been compared with previously studied hairpins with three and four residues in the loop and surprising agreements in the NOE patterns and resulting overall folding have been observed. It would be very interesting to gain a better quantitative understanding of the transition between the T7- and T8-hairpin.

ACKNOWLEDGMENT

NMR spectra were recorded at the Dutch National Hf-NMR Facility (Nijmegen, the Netherlands) supported by SON. We wish to thank Ing. J. van Os and Ing. J. Joordens for technical assistance.

REFERENCES

Baxter, S. M., Greizenstein, M. B., Kushlan, D. M., & Ashley, G. W. (1993) *Biochemistry 32*, 8702–8711.

Blommers, M. J. J., Haasnoot, C. A. G., Hilbers, C. W., van Boom, J. H., & van der Marel, G. A. (1987) *Struct. Dyn. Biopolym., NATO ASI Ser. E: Appl. Sci. 133*, 78–91.

Blommers, M. J. J., Haasnoot, C. A. G., Walters, J. A. L. I., van der Marel, G. A., van Boom, J. H., & Hilbers, C. W. (1988) *Biochemistry 27*, 8361–8369.

Blommers, M. J. J., Walters, J. A. L. I., Haasnoot, C. A. G., van der Marel, G. A. van Boom, J. H., & Hilbers, C. W. (1989) *Biochemistry 28*, 7491–7498.

Blommers, M. J. J., van de Ven, F. J. M., van der Marel, G. A., van Boom, J. H., & Hilbers, C. W. (1991) *Eur. J. Biochem. 201*, 33–51.

Boulard, Y., Gabarro-Arpa, J., Cognet, J. A. H., LeBret, M., Guy, A., Téoule, R., Guschlbauer, W., & Frazakerley, G. V. (1991) *Nucleic Acids Res. 19*, 5159–5167.

Cantor, C. R., & Schimmel, P. R. (1980) *Biophysical Chemistry, Part II*, W. H. Freeman and Company, San Francisco.

Chazin, W. J., Wütrich, K., Hyberts, S., Rance, M., Denny, W. A. & Leupin, W. (1986) *J. Mol. Biol. 190*, 439–453.

Güntert, P., Braun, W., & Wüthrich, K. (1991) *J. Mol. Biol. 217*, 517–530.

Haasnoot, C. A. G., & Hilbers, C. W. (1983) *Biopolymers 22*, 1259–1266.

Haasnoot, C. A. G., de Bruin, S. H., Berendsen, R. G., Janssen, H. G. J. M., Binnendijk, T. J. J., Hilbers, C. W., van der Marel, G. A., & van Boom, J. H. (1983a) *J. Biomol. Struct. Dyn. 1*, 115–129.

Haasnoot, C. A. G., Westerink, H. P. van der Marel, G. A., & van Boom, J H. (1983b) *J. Biomol. Struct. Dyn. 1*, 131–149.

Haasnoot, C. A. G., Hilbers, C. W., van der Marel, G. A., van Boom, J. H., Singh, U. C., Pattabiraman, N., & Kollman, P. A. (1986) *J. Biomol. Struct. Dyn. 3*, 843–857.

Hare, D. R., Wemmer, D. E., Chou, S.-H., Drobny, G., & Reid, B. R. (1983) *J. Mol. Biol. 171*, 319–336.

Jeener, J., Meier, B. H., Bachmann, P., & Ernst, R. R. (1979) *J. Chem. Phys. 71*, 4546–4553.

Johnson, D., & Morgan, A. R. (1978) *Proc. Natl. Acad. Sci. U.S.A. 75*, 1637–1641.

Keepers, J. W., & James, T. L. (1984) *J. Magn. Res. 57*, 404–426.

Larsen, A., & Weintraub, H. (1982) *Cell 29*, 609–622.

Lyamichev, V. I., Mirkin, S. M., & Frank-Kamenetskii, M, D. (1985) *J. Biomol. Struct. Dyn. 3*, 327–338.

Marion, D., & Wüthrich, K. (1983) *Biochim. Biophys. Res. Commun. 113*, 967–974.

Mooren, M. M. W. (1993) Thesis, University of Nijmegen.

Mooren, M. M. W., Pulleyblank, D. E., Wijmenga, S. S., Blommers, M. J. J., & Hilbers, C. W. (1990) *Nucleic Acids Res. 18*, 6523–6529.

Orbons, L. P. M., van der Marel, G. A., van Boom, J. H., & Altona, C. (1986) *Nucleic Acids Res. 14*, 4187–4196.

Orbons, L. P. M., van Beuzekom, A. A., & Altona, C. (1987) *J. Biomol. Struct. Dyn. 4*, 965–987.

Pieters, J. M. L., de Vroom, E., van der Marel, G. A., van Boom, J. H., Koning, T. H. G., Kaptein, R., & Altona, C. (1989) *Biochemistry 29*, 788–799.

Pulleyblank, D. E., Haniford, D. B., & Morgan, A. R. (1985) *Cell 42*, 271–280.

Saenger, W. (1984) *Principles of Nucleic Acids Structure*, Springer Verlag, New York.

Sarma, H., Mynott, R. J., Wood, D. J., & Hruska, F. E. (1973) *J. Am. Chem. Soc. 95*, 6457–6459.

Scheek, R. M., Russo, N., Boelens, R., Kaptein, R., & van Boom, J. H. (1983) *J. Am. Chem. Soc. 105*, 2914–2916.

van de Ven, F. J. M., Blommers, M. J. J., Schouten, R. E., & Hilbers, C. W. (1991) *J. Magn. Res. 94*, 140–151.

Wells, R. D., Collier, D. A., Hanvey, J. C., Shimizu, M., & Wohlrab, F. (1988) *FASEB J. 2*, 2939–2949.

Wijmenga, S. S., Mooren, M. M. W., & Hilbers, C. W. (1993) in *NMR of Macromolecules, A Practical Approach* (Roberts, G. C. K., Ed.) pp 217–288, Oxford University Press, Oxford.

Wohlrab, F., McLean, M. J., & Wells, R. D. (1987) *J. Biol. Chem. 262*, 6407–6416.

Wüthrich, K. (1986) *NMR of Proteins and Nucleic Acids*, Wiley and Sons, New York.